Adsorption potentials for nonplanar geometries

A. Hernando,[1] E. S. Hernández,[2] R. Mayol,[1] and M. Pi[1]

[1] *Departament d'Estructura i Components de la Matèria, Facultat de Física, and IN^{2}UB, Universitat de Barcelona, 08028 Barcelona, Spain*

[2] *Departamento de Física, Facultad de Ciencias Exactas y Naturales, Universidad de Buenos Aires and Consejo Nacional de Investigaciones Científicas y Técnicas, Argentina*

(Dated: July 11, 2007)

Abstract

We present a method to compute, assuming a continuous distribution of sources, the elementary potential created by a differential element of volume of matter, whose integral generates a known adsorption field $V(z)$ for a planar surface. We show that this elementary potential is univocally determined by the original field and can be used to generate adsorption potentials for other nontrivial geometries. We illustrate the method for the Chizmeshya-Cole-Zaremba physisorption potential and discuss several examples and applications.

PACS numbers: 68.08.Bc,68.08.-p,68.65.-k,68.35.Np

I. INTRODUCTION

One important field of research in low temperature physics is adsorption of quantum fluids on surfaces of various geometries. For most nontrivial shapes of the substrate, the lack of a reliable and easy-to-use adsorption potential represents a serious limitation for calculational purposes. Traditionally, this difficulty has been sorted out in essentially two ways. One is to compute the integral of a threedimensional (3D) adatom-adsorber pairwise interaction over the specified geometry, as carried out for planar,[1–6] cylindrical[7] and spherical[8] substrates. The other approach, oriented to geometries presenting angles –*i.e*, wedges and polygonal pores– is to compose the adsorbing field by summing up the contributions from the participating walls.[9–13] While the former procedure is of limited accuracy in the case of highly structured substrates such as graphite, the second can be shown to overestimate the adsorption strength near vertices due to double–counting from the region where the half–solids overlap. Notwithstanding these limitations, the physics of confined quantum fluids has largely benefited from the various approximations to trace general trends and anticipate on several interesting phenomena, such as prewetting transitions on planar substrates, and pore and wedge filling. However, the choice of the force parameters such as well depth and interaction range are critical when determining characteristics of film growth, atom dynamics and phase diagram of the adsorbed fluid.[12] It is then useful to develop a tool to derive the most accurate, trustworthy potential for the given confining, nonplanar environment.

The Chizmeshya-Cole-Zaremba (CCZ) physisorption potential[14] for noble gases and hydrogen on metal surfaces is, up to now, the best suited for studies of wetting of planar substrates. These authors have provided the field $V_{CCZ}(z)$ created by a semiinfinite solid material at distance z from the free surface. The construction of this family of potentials is carried out by adding dispersion and overlap contributions, both determined ab initio. The result is then fit to a simple functional form, namely

$$V_{CCZ}(z) = V_0\,(1+\alpha z)\,e^{-\alpha z} - f_2\left[\beta(z)\,(z-z_{vdW})\right]\,\frac{C_{vdW}}{(z-z_{vdW})^3} \qquad (1)$$

with $f_2(x) = 1 - e^{-x}\,(1 + x + x^2/2)$ and $\beta(z) = \alpha^2 z/(1+\alpha z)$, which is used in this paper. In view of its physical origin and analytical form, this potential cannot, in principle, be decomposed as a summation over pair interactions between adsorbate and atoms in the adsorber. However, we may intuitively think on purely geometrical grounds that, if all the differential volume elements in the material contribute to the adsorption potential at z with

a weight depending only on the distance to the adatom, the total strength $V_{CCZ}(z)$ can be obtained by an integration over a continuous half-solid. In such a case, one can design a method to obtain that elementary potential from the adsorption field.

In this work, we show that given a physisorption potential for a planar surface, of the form $V(z)$, under very general assumptions it is possible to decompose it into contributions from elementary geometric sources located in the bulk of the material. Once these generators are identified, appropriate recombination into an integral for an arbitrary geometry permits to simulate a distortion of the original planar surface and obtain the corresponding two– or threedimensional adsorption potential. The general method is described in Sec. II. In Sec. III we present several illustrations of the general procedure and discuss aspects of the condensation of helium in various geometries. The conclusions and perspectives are summarized in Sec. IV.

II. THE METHOD

For arbitrary geometries, the potential V created by a continuous distribution of matter $\rho(\mathbf{r}')$ on an atom placed at $\mathbf{r} = (x, y, z)$ is given by the convolution

$$V(\mathbf{r}) = \int d\mathbf{r}'\, \rho(\mathbf{r}')\, v(\mathbf{r}' - \mathbf{r}), \tag{2}$$

where the generating kernel $v(\mathbf{x})$ is defined here as the *elementary potential*. For a continuous half-solid with free surface at position $z' = 0$, we have $\rho(\mathbf{r}') = \rho_0\, \Theta(-z')$, where ρ_0 is the bulk density of the material and $\Theta(x)$ the usual Heavyside function. Hereafter, we adopt a reference potential $V_{ref}(z)$ –for example, the CCZ one– and assuming that v depends only on the distance, the integral is

$$V_{ref}(z) = \rho_0 \int_{-\infty}^{\infty} dx' \int_{-\infty}^{\infty} dy' \int_{z}^{\infty} d\zeta\, v(R) \tag{3}$$

with $\zeta = z - z'$, $R = \sqrt{x'^2 + y'^2 + \zeta^2}$. In this expression we have explicitly taken advantage of the translational invariance of the system on the horizontal plane.

Choosing polar coordinates (r', φ') in the (x', y') plane, Eq. (3) becomes

$$V_{ref}(z) = 2\pi\, \rho_0 \int_{z}^{\infty} d\zeta \int_{\zeta}^{\infty} dR\, R\, v(R) \tag{4}$$

The latter line indicates that in this case the elementary sources for the potential at z are parallel planes in the bulk of the adsorber, at vertical distance ζ from the test particle.

Other selection of coordinates allows one to identify sources of various shapes such as parallel filaments and cylindrical or spherical surfaces. Moreover, since Eq. (4) is an integral equation to be solved under adequate boundary conditions, it can be proven that if $v(R)$ is requested to vanish at infinity, it is unique.

For this sake, we note that double differentiation of Eq. (3) with respect to z gives

$$V''_{ref}(z) = 2\pi\,\rho_0\,z\,v(z) \tag{5}$$

In fact, this is a representation of Poisson's equation for the distribution of elementary sources: computing the Laplacian of the convolution equation (2) and switching integration variables, one has

$$\nabla^2 V(\mathbf{r}) = \int d\mathbf{r}'\nabla^2\rho(\mathbf{r}-\mathbf{r}')v(\mathbf{r}') \tag{6}$$

Introducing the matter density of a semiinfinite solid, the above equation becomes

$$\frac{d^2V_{ref}(z)}{dz^2} = \int d\mathbf{r}'\delta'(z-z')v(\mathbf{r}') \tag{7}$$

Integration by parts with appropiate choice of variables immediatly leads to Eq. (5), which clearly shows that for a given $V_{ref}(z)$, the elementary potential is univocally and simply defined; it naturally satisfies the necessary boundary condition of vanishing at large distances [cf. Eq. (1)] and can be applied to arbitrary geometries, writing the distance R between adatom and adsorber in an adequate coordinate system and multiplying by the proper weighting function. Computationally, Eq. (5) and the subsequent integration given by (4) is very fast and precise.

For matter with constant density ρ_0 and an arbitrary surface defined by a function $z = f(x,y)$, Eqs. (2) and (5) give the potential $V(\mathbf{r})$ on a test particle as

$$V(\mathbf{r}) = \int \frac{d\mathbf{r}'}{2\pi}\,\Theta\left[f(x',y')-z'\right]\,\frac{V''_{ref}(|\mathbf{r}-\mathbf{r}'|)}{|\mathbf{r}-\mathbf{r}'|} \tag{8}$$

In particular, the restriction to a half–solid

$$V_{ref}(z) = \int \frac{d\mathbf{r}'}{2\pi}\,\Theta\left[-z'\right]\,\frac{V''_{ref}(|\mathbf{r}-\mathbf{r}'|)}{|\mathbf{r}-\mathbf{r}'|} \tag{9}$$

permits to define the 'planar potential' $V(z)$ as a solution of this integral equation. It is straighforward to prove that the widely used 3–9 potentials derived from the LJ pair interaction[1–6,10–12] belong to this class.

	He		H_2	
Species	$\rho_0\, v_{CCZ}(r_{min})$ (KÅ^{-3})	r_{min} (Å)	$\rho_0\, v_{CCZ}(r_{min})$ (KÅ^{-3})	r_{min} (Å)
Mg	-0.214	4.72	-1.556	4.03
Li	$-7.22\ 10^{-2}$	5.38	-0.544	4.60
Na	$-4.31\ 10^{-2}$	5.65	-0.324	4.82
K	$-2.04\ 10^{-2}$	6.17	-0.153	5.25
Rb	$-1.67\ 10^{-2}$	6.33	-0.125	5.37
Cs	$-1.55\ 10^{-2}$	6.34	-0.117	4.97

TABLE I: Minimum of the elementary CCZ potential and its position for a He atom and a H_2 molecule.

As a first test, we have computed the elementary potentials $v_{CCZ}(r)$ corresponding to the CCZ adsorption fields for He atoms and H_2 molecules on various metallic substrates. The minimum values $v_{CCZ}(r_{min})$ and their positions are listed in Table I and the elementary potentials are plotted in the upper panel of Fig. 1. The lower panel shows the CCZ potentials (full lines) together with the elementary potentials integrated according to Eq. (4) using a Gauss quadrature (symbols). From this figure, it can be seen that the original CCZ potential is recovered after integration over continuous differential elements of matter.

It should be noted that one limitation of the method may appear in the fact that $v_{CCZ}(R)$ is negative for $\alpha R < 1$ (cf. Eq. (1)). This is not visible in the scale of Fig. 1 (a) since for all metals in Table I, the short–range parameter α lies between 0.5 and 0.7 Å; the striking convergence among points and lines in Fig. 1(b) indicates that this apparent drawback is irrelevant upon integration over large samples of matter. Similarly, the long–range scale z_{vdW} of the CCZ potentials –between 0.19 and 0.34 Å – introduces another limitations. Given these two natural lenghts of the CCZ potentials, and their typical values, it appears that the present method can be safely employed insofar as integrations are carried over samples of matter larger than around 2 Å.

III. SOME RESULTS FOR HE ADATOMS

We have performed integrations of the elementary CCZ potentials for helium atoms for a variety of shapes. In current research of wetting by quantum fluids, interesting geometries are hollow cylinders of infinite length with different transverse sections, that simulate pores inside bulk material. For circular cylinders, the potentials have been computed from LJ pair interactions[7] and for geometries including angles, such as the hexagonal pore in Refs. 10,12, the confining field has been represented as the summation of six 3–9 potentials. In addition, a cusp of solid material may provide a tool to model some irregularities on rough surfaces. As an illustration, in the lower and upper panels of Fig. 2 we respectively display the (x, z) contour plot of the integrated potential for a Cs solid cusp and for an hexagonal pore in bulk Cs, in both cases with translational invariance along the y–axis. It is interesting to note that the hexagonal pore field can be computed summing six nonoverlapping solid cusps, with walls indicated by the dotted lines in the plot. The potential landscapes clearly reveal the expected condensation patterns, that for small amounts of helium, consist of one quasi–twodimensional layer on either cusp wall and of one quasi–one dimensional stripe at each vertex of the hexagon. The latter is consistent with the condensation pattern encountered in Ref. 12.

In Fig. 3, we show the potentials inside infinite cylindrical cavities of radius $R = 10$ Å in bulk Cs, Li and Mg, plotted as a function of radial distance, together with those computed as in Ref. 16 out of integration of a LJ potential. The parameters ε and σ from Ref. 8 have been fixed so as to reproduce the depth of the corresponding planar CCZ field. We note that although quite similar in shape and scales, the CCZ–based potentials for the strong adsorbers Li and Mg are moderately deeper and the minima are slightly shifted out of the tube wall, as compared with the LJ ones.

The method here proposed can demonstrate that for pores with polygonal section, the summation of planar potentials may be a reliable approximation far from a vertex, whereas they overestimate the adsorption strength substantially in the vicinity of an apex. As an illustration, we consider a rhombic pore with angles of 60° and 120°, extending infinitely along the y-axis in bulk Cs. Since such a pore can be viewed as a symmetric array of two wedges of finite height, forming four inner apertures, it is clear that for small amounts of helium, one should expect condensation near the vertices. In order to visualize the

enhancement of the physisorption strength, in Fig. 4 we represent the integrated elementary potential, together with the summation of four planar CCZ fields, along the diagonals of pores with side of 20 and 50 Å, respectively in the upper and lower panels. We realize that the overestimation effects are sizable at the weakest minima corresponding to the vertices joined by the shortest diagonal, where the depth is increased by 5–6 K, as opposed to less than 2 K in the large diagonal of the small pore. The potentials are essentially indistinguishable along the longest diagonal of the large pore.

Another interesting illustration is a 3D conical pore. Figure 5 shows the equipotential lines of such structure on the (r, z) plane, for apertures of 120º and 60º, and a depth of 50 Å. This potential landscape on a symmetry plane is qualitatively similar to that corresponding to a linear wedge with finite height, and far enough from the pore, we recover the CCZ potential of the planar surface. This example combines a wedge-like and a cusp-like behavior, as seen in the contours, and indicates that within vertical heights of the order of the position of the minimum, where condensation of the adsorbate takes place for not too large amounts of helium, boundary effects can be safely neglected.

Finally, we revise the problem of condensation of helium in wedges.[13] In Fig. 6 we illustrate the density profile along the z- axis (upper panel) and the equidensity lines corresponding to half the saturation density of ^{4}He (lower panel) in an infinite wedge with aperture of 170º, for a linear density of 140 Å^{-1}. Full and dotted lines correspond to the wedge potential generated by the elementary CCZ sources and to the summation of two planar CCZ fields as done in Ref. 13. We see in the upper figure that double counting at the apex enhances the height of the main peak by nearly 25% and compresses the sample on the vertical axis by 2-3 Å. This enhancement is totally attributed to the extra attraction near the vertex provoked by the overlapping planes. Both representations of the potential agree in the location of the density peaks and coincide at the minima of the density oscillations. The shape of the sample in the lower plot also shows an overall compresion of the meniscus, compensated by some spreading of the helium fluid near the contact line. Note that for this large opening, double counting effects in the density profiles, however moderate, are visible; a similar comparison carried at *i.e.*, 45º gives almost indistinguishable fluid distributions. This behavior is supported by a glance at the energetic features displayed in Table 2, where we show the energy per particle, chemical potential and grand potential per particle $\Omega/N = E/N - \mu$ for helium atoms on planar Cs and on Cs wedges of 170º and 45º, the latter

computed under the summation approximation and by integration of the CCZ elementary potentials.

Aperture	$E/N(K)$	$\mu(K)$	Ω/N
180^o	-7.07	-7.13	0.06
170^o (Integrated CCZ)	-7.08	-7.13	0.05
170^o (Two CCZ planes)	-7.29	-7.16	-0.13
45^o (Integrated CCZ)	-7.42	-7.31	-0.12
45^o (Two CCZ planes)	-7.42	-7.31	-0.12

TABLE II: Energy per particle, chemical potential and grand potential per particle for helium atoms on planar Cs and on Cs wedges of 170^o and 45^o, computed by integration of the CCZ elementary potentials and by summation of two planar CCZ potentials.

These results show that folding a plane into an angle of 170^o is, in fact, a minor perturbation provided that the adsorption field is properly computed, since all relevant energetic features remain essentially unchanged. By contrast, the summation of two planar fields is a poor approximation that changes the wetting behaviour from nonwetting ($\Omega/N > 0$) to wetting ($\Omega/N < 0$). Instead, for a not–too–small angle such as 45^o both representations of the adsorption field yield equivalent results. This identity between results provided by the two different representation of the wedge potential persists for even smaller angles at which bridge configurations of the helium atoms appear.[13] It is also worth noting that in the present calculation, for either potential, all wedge configurations are thermodynamically stable with respect to a droplet with same linear density lying on one planar wall (aperture of 180^o), since the latter carries the highest (nonwetting) grandpotential per particle. These properties are important in view of the different adsorption isotherms at fixed angle[15] that can be expected under these two methods; an inadequate choice of the potential might shift the condensation threshold to lower linear densities in the wedge. This is the case for hexagonal silica and metallic pores.[18] In particular, the approximation under which the calculations in Ref. 13 were performed is perfectly reliable, since only the aperture range below 120^o, where the interesting phenomena concerning filling and emptying transitions appear to take place, was there considered.

IV. SUMMARY

In this work we have proposed a means to derive the elementary potentials that create a given planar adsorption potential, assumming a continuous distribution of the sources. The output can afterwards be integrated weighted with a density that corresponds to an arbitrary geometry, to obtain the adsorption potential for a semiinfinite solid with a nonplanar solid–fluid interface. The method is numerically fast and robust, and gives rise to potential landscapes that account adequately for the irregularities of the surface, as viewed in several illustrations presented in this work. For specific geometries with particular invariances, the integration involves one or two dimensions, and eventually reduces either partially or totally to some analytical expression.

All applications presented in this paper invoke one class of planar potentials, the CCZ ones, derived for metallic substrates. These are *ab initio* potentials that cannot, in principle, be representated by summation or integration of a pair interaction between adatom and adsorbate atom over the substrate. However, in many situations of experimental and theoretical interest, the material exposed to the helium vapor is a glass or a gel of silica strands.[6,11,12] In these cases, the only planar adsorption potential available is the 3–9 one, and the adopted procedure to derive the field inside a polygonal pore is summation of planes.[10,12] Integration of the elementary potential, which for the 3–9 field amounts to integrating the original LJ pair interaction, as shown in this paper, could improve substantially the description avoiding undesired double–counting effects in the vicinity of vertices.[18]

Some of the geometries presented here as illustrations can be viewed as 'folding' or deformations of a planar interface. With the construction of a cusp and a conical pore, we show that with this procedure one can mimic irregularities in a planar substrate, where approximations based on summation of planar potentials cannot be applied. This is especially promising with the perspective of modelling rough or patterned surfaces[17] keeping the most important physical characteristics of the planar one that gives rise to the elementary potential.

Acknowledgements

We are indebted to Francesco Ancilotto, Manuel Barranco and Milton Cole for helpful discussions and useful comments on this manuscript. This paper was performed under grants No. FIS2005-01414 MEC-DGI and 2005SGR00343 Generalitat de Catalunya (Spain), PIP 5138/05 from CONICET and X298 from University of Buenos Aires (Argentina).

---

[1] E. Cheng, M. W. Cole, W. F. Saam and J. Treiner, Phys. Rev. Lett. **67**, 1007 (1991).

[2] N. Pavloff and J. Treiner, J. Low Temp. Phys. **83**, 331 (1991).

[3] E. Cheng, M.W. Cole, W.F. Saam and J. Treiner, Phys. Rev. B **48**, 18214 (1993).

[4] E. Cheng, M.W. Cole, J. Dupont-Roc, W.F. Saam and J. Treiner, Rev. Mod. Phys. **65**, 557 (1993).

[5] J. Treiner, J. Low Temp. Phys. **92**, 1 (1993).

[6] V. Apaja and E. Krotscheck, Phys. Rev. B **67**, 184304 (2003); Phys. Rev. Lett. **91**, 225302 (2003).

[7] G. Stan and M. W. Cole, Surf. Sci. **395**, 280 (1998).

[8] E. S. Hernández, M. W. Cole and M. Boninsegni, Phys. Rev. B **68**, 125418 (2003).

[9] E. Cheng and M.W. Cole, Phys. Rev. B **41**, 9650 (1990).

[10] M.W. Cole, F. Ancilotto and S. M. Gatica, J. Low Temp. Phys. **138**, 195 (2005).

[11] M. Rossi, D. E. Galli and L. Reatto, J. Low Temp. Phys. **146**, 95 (2006).

[12] M. Rossi, D. E. Galli and L. Reatto, Phys. Rev. **72**, 064516 (2005).

[13] E. S. Hernández, F. Ancilotto, M. Barranco, R. Mayol and M. Pi, Phys. Rev. B **73**, 245406 (2006).

[14] A. Chizmeshya, M. W. Cole, and E. Zaremba, J. Low Temp. Phys. 110, 677 (1998).

[15] R. Mayol, F. Ancilotto, M. Barranco, E. S. Hernández and M. Pi, J. Low Temp. Phys. (2007), in print.

[16] E. S. Hernández, J. Low Temp. Phys. **137**, 89 (2004).

[17] J. Klier, P. Leiderer, D. Reinelt, and A.F.G. Wyatt, Phys. Rev. B **72**, 245410 (2005).

[18] E. S. Hernández, A. Hernando, R. Mayol and M. Pi, *Proceedings of the 14th International Conference on Recent Progress in Many–Body Theory*, Barcelona, Spain, July 2007 (to be

published).

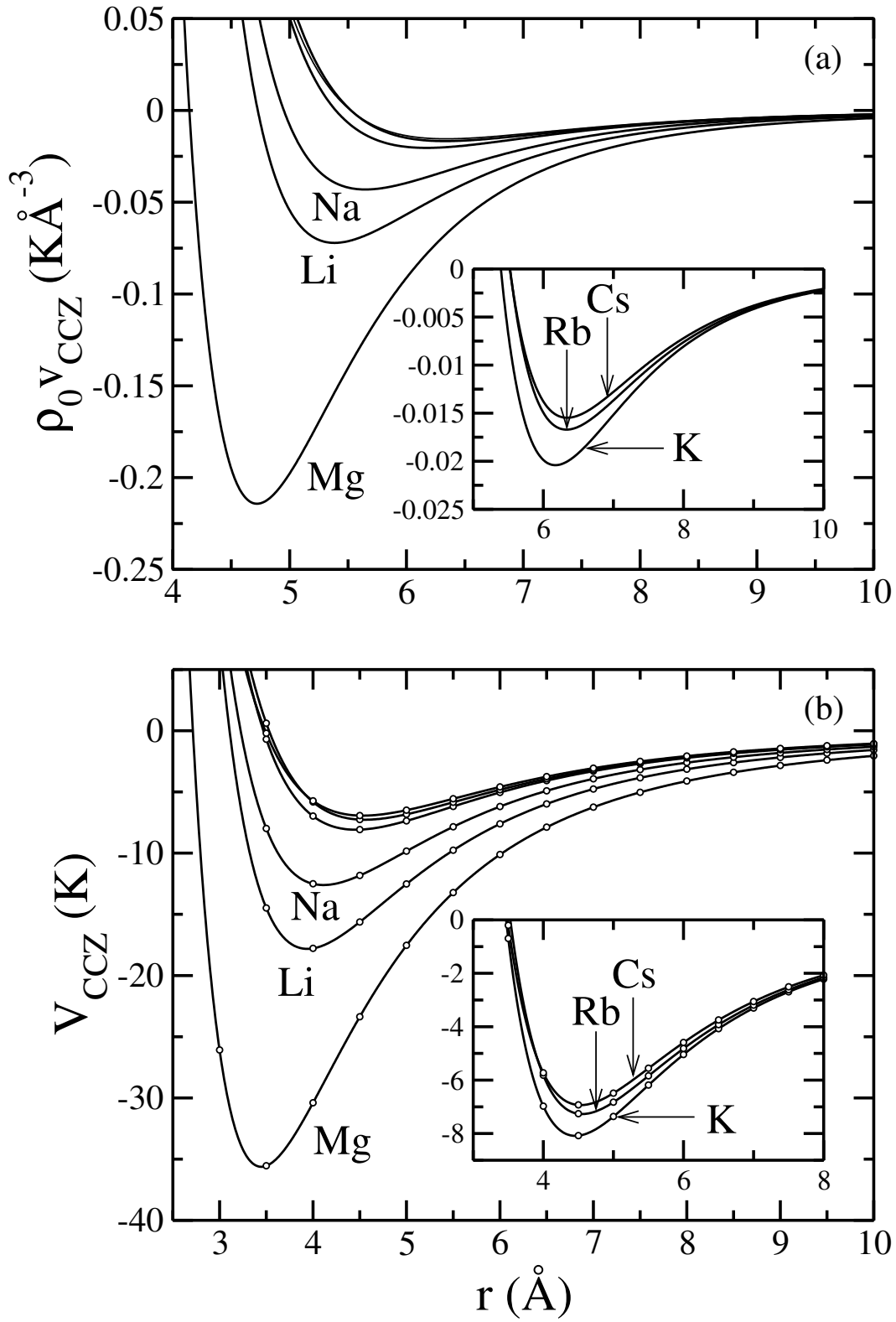

FIG. 1: (a) Elementary potential $\rho_0\, v_{CCZ}(r)$ for a He atom in the presence of several metal substrates; (b) the CCZ potentials (full lines) and the integrals of the elementary potentials from the upper plot (symbols). The insets span the neighborhood of zero potential.

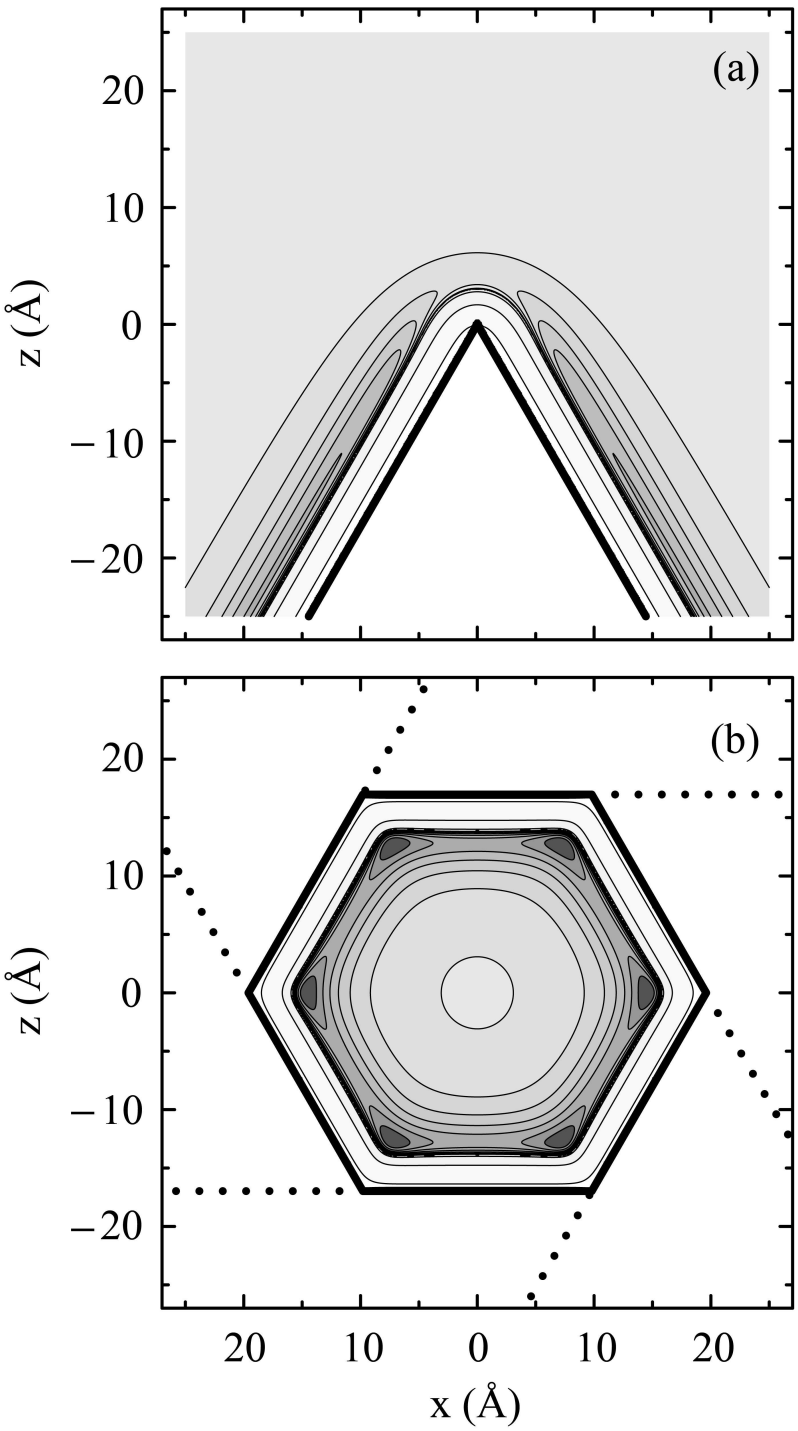

FIG. 2: (a) Potential landscape for an infinite Cs cusp; (b) same for an infinite hexagonal pore in bulk Cs. The solid walls are indicated with dark lines.

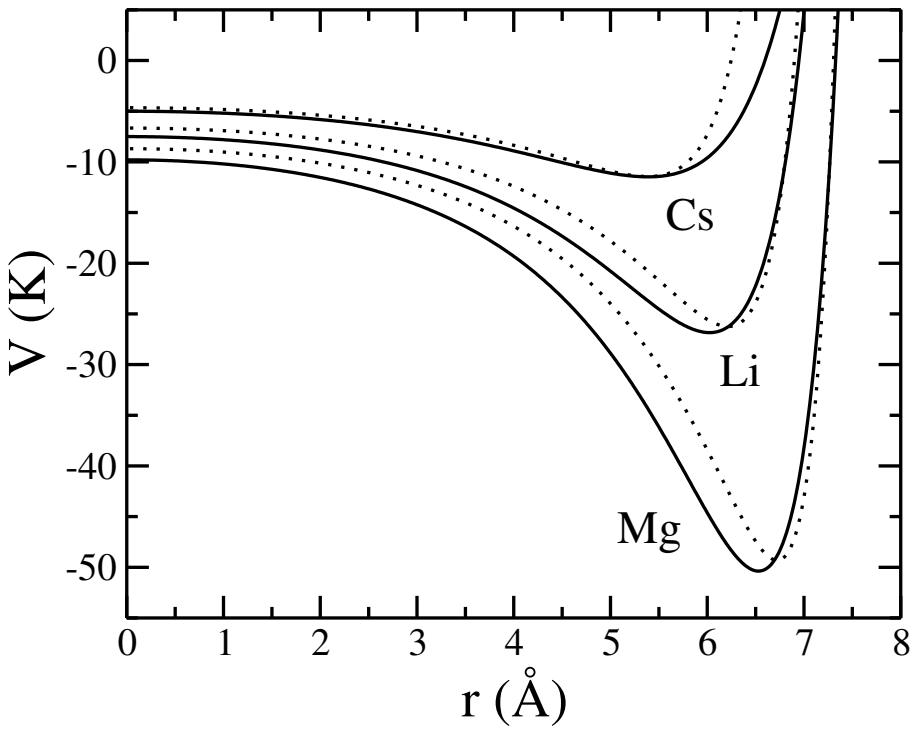

FIG. 3: Integrated CCZ potentials for a He atom inside infinite cylindrical pores of radius $R =$ 10 Å in bulk Cs, Li and Mg, compared with the ones derived from a LJ pair interaction (full and dotted lines, respectively).

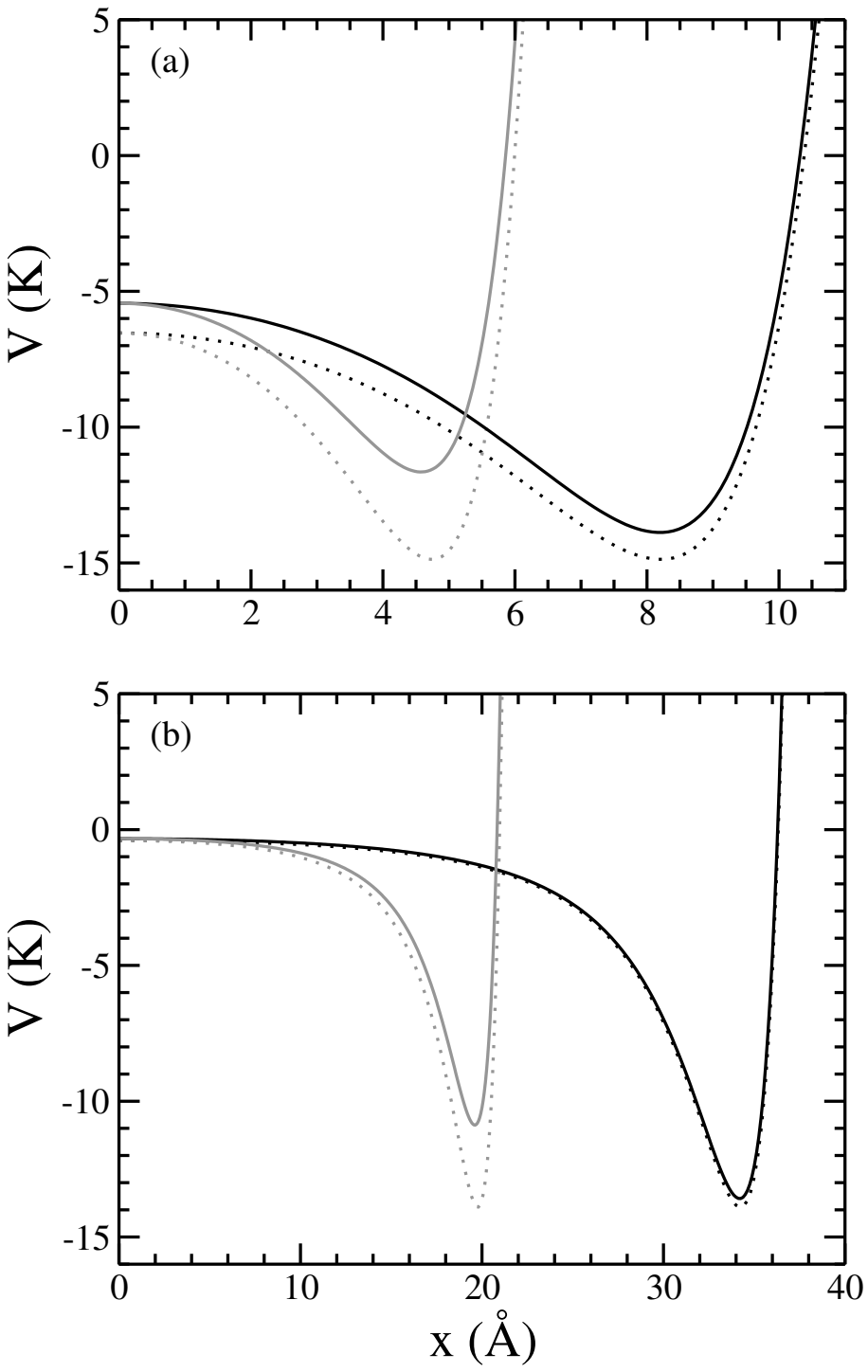

FIG. 4: Integrated elementary potential $V_{rhombus}(x, z)$ along the diagonals of a hollow rhombus of side (a) 20 Å and (b) 50 Å, both with angles of 60° and 120° in bulk Cs (full lines), compared with the adsorption potential generated by four planar CCZ fields at the indicated angles (dotted lines). The coordinate origin is at the center of the rhombus and x is the distance along each diagonal. Dark (grey) curves correspond to the longest (shortest) diagonal.

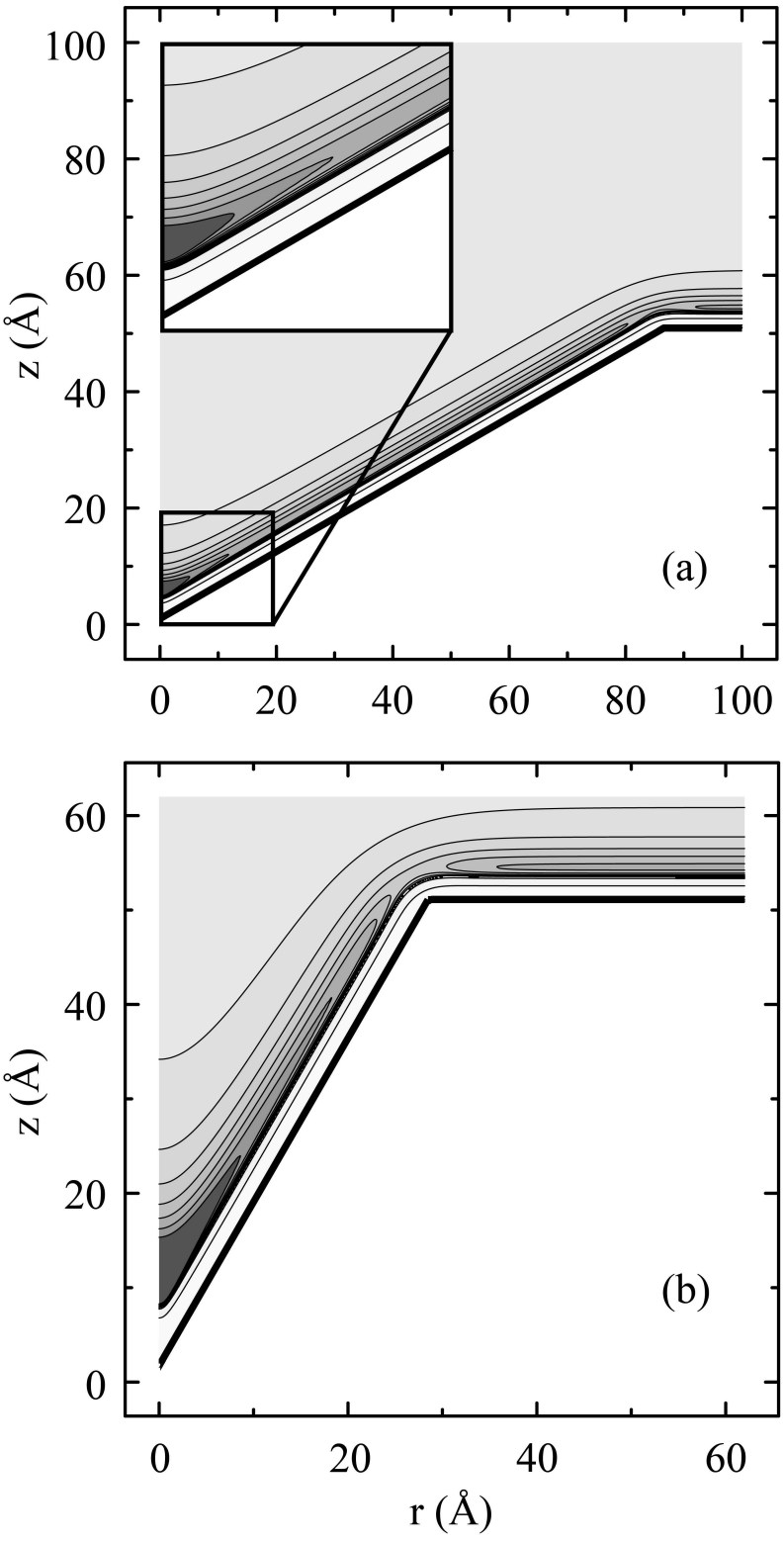

FIG. 5: Integrated potential $V_{cone}(r, z)$ for a conical hole with 50 Å depth on a symmetry plane. (a) Aperture of 120°; (b) aperture of 60°.

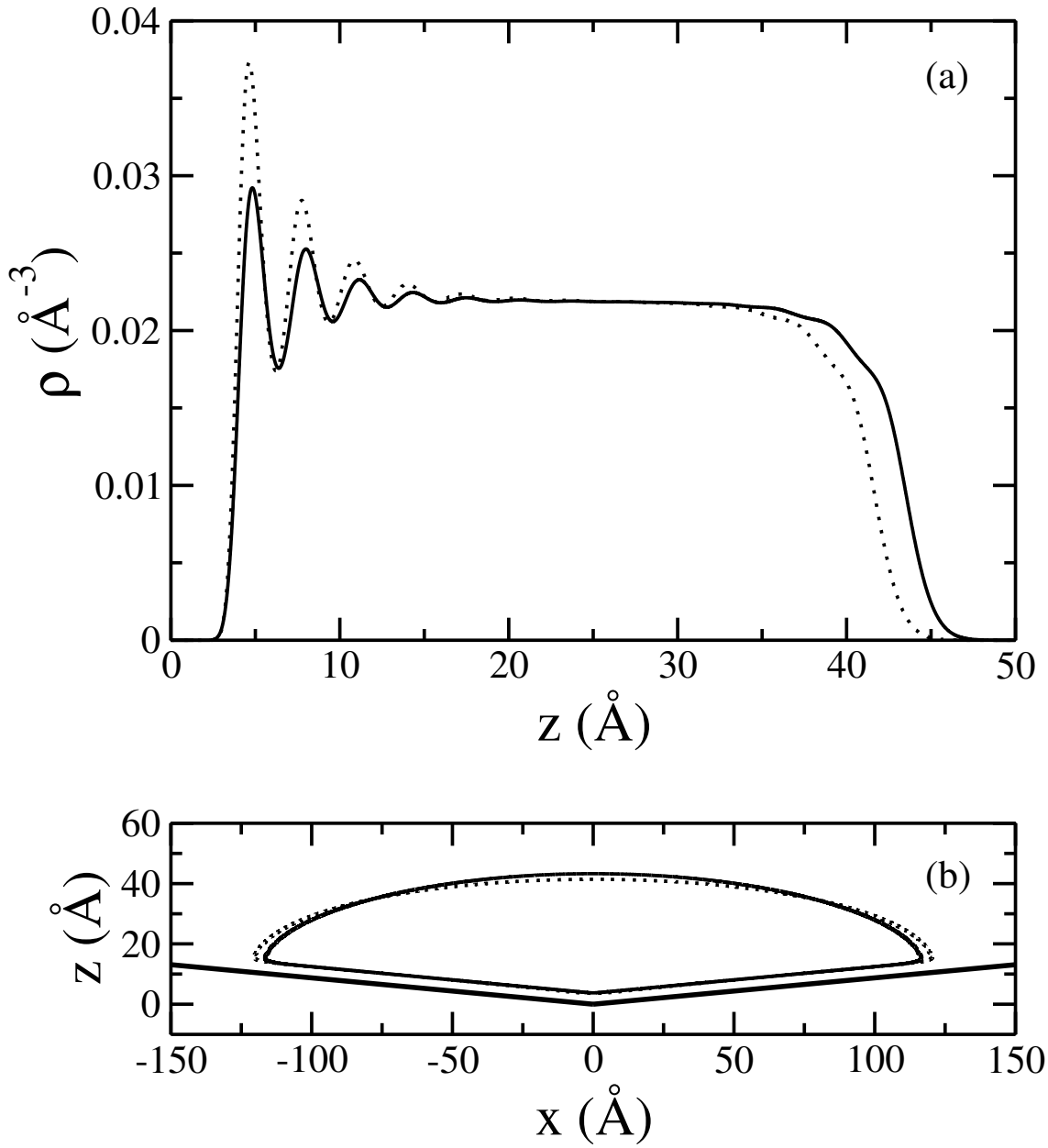

FIG. 6: (a) Density profile on the z- axis of a wedge with aperture of 170°; (b) equidensity contour at half the saturation density of bulk ^{4}He. Full and dotted lines respectively correspond to the integrated CCZ elementary potential and to the summation of two planar CCZ potentials. The linear atom density is 140 Å^{-1}.